A MEMS FABRICATION TECHNIQUE FOR NON-PLANAR SUBSTRATES

Wen J. Li*, John D. Mai†, and Chih-Ming Ho†

* *Department of Mechanical and Automation Engineering, The Chinese University of Hong Kong*
Room 617, Ho Sin-Hang Eng. Bldg., Shatin, New Territories, Hong Kong
wen@mae.cuhk.edu.hk

† *Department of Mechanical and Aerospace Engineering, University of California at Los Angeles*
Room 44-121, Eng. IV Bldg., Los Angeles, CA, 90095

ABSTRACT

The integration of MEMS sensors, actuators, and IC devices onto macro mechanical parts is a critical technology necessary for the potential realization of intelligent mechanical structures. The current planar fabrication methods offered by the MEMS/IC industry restrict the possibility of integrating micro devices onto contoured (non-planar) mechanical structures. We have developed a lithographic technique to directly fabricate micron-sized sensing and actuation structures onto a cylindrical surface. This novel technology includes the development of flexible masks, photoresist spraying technique, and customized alignment systems. Results indicate that line resolution of <5μm is possible for structures on the surface of a 2" (5.08cm) long cylinder with a diameter of 1.25" (3.175cm). This paper describes the procedures developed to fabricate sacrificially release micro structures onto a cylindrical surface. The performance of some micro thermal actuators and shear stress sensors on a quartz cylindrical substrate are also presented.

INTRODUCTION

Attempts to create macromachines that can sense and control their environment are underway. Sensing very complex physical phenomena such as turbulent shear stress using MEMS sensors and the control of skin friction by MEMS actuators have already been demonstrated by Ho et al. in 1994 [1]. Currently, the total integration of sensors, actuators, and decision making IC components for flow control are under investigation by CIT/UCLA [2]. Besides aerodynamic flow control and monitoring, other proposed applications for integrated MEMS-mechanical systems are condition-based maintenance, environmental monitoring, process control, robotics, and automation [3,4]. Since standard MEMS//IC process technology only allows the fabrication of microstructures on flat substrates, the MEMS/IC components must reside on a flat chip. Typically, the micromachined devices are implanted onto mechanical surfaces that are pre-machined with recesses to contain the devices [1]. Other methods include fitting hermetically sealed sensor and circuit system into machined parts [3]. Thus, the packaging of chips onto macro mechanical parts often changes the contour of the macro substrates, which, in some cases, can be detrimental to the function of the macro components. For instance, changing the leading edge contour of an airfoil can significantly decrease lift on the airfoil.

Methods such as epitaxial lift-off [5] and total-substrate- removal [6] were developed to put optical/electronic devices such as diode lasers and HEMTs (high electron mobility transistors) on flexible substrates that can be bonded to arbitrary substrates. Using similar techniques, CIT/UCLA have fabricated surface-micromachined shear stress sensors on flexible substrates that can be conformed to non-planar macro mechanical parts [7]. The flexible-substrate method offers the advantage of producing functional devices using a fully IC compatible process. However, this approach lacks the capability to *bulk-micromachine* contoured mechanical substrates. Also, glue uniformity, stress induced by the glue on the film, and alignment of the films to a desired orientation are some of the issues to be addressed when this approach is used.

Other methods such as direct-write [8], flexible stamp [9], direct-tooling [10], and shadow-masking can also be used to produce microstructures on a contoured surface. However, to the best of our knowledge, no work has reported a procedure to align multiple layers of images or produced sacrificially released microstructures on a macro non-planar surface.

THE FLEXIBLE MASK TECHNIQUE

We have developed a technique to directly fabricate sacrificially released micro sensors and actuators onto the surface of a macro cylindrical substrate. The important aspects of this technique are the development of the flexible masks (FM) and a method to correct alignment errors.

Flexible Masks

A flexible UV-transparent material can be used as a flexible mask that conforms to non-planar surfaces if non-UV-transparent micron-sized structures can be patterned on it. As illustrated in Figure 1, non-UV-transparent thinfilms such as Cr or Au can be evaporated onto a flexible material and then patterned using conventional microlithographic procedures such as spin-on photoresist and contact UV exposure. Hence, the image resolution on the flexible masks has the theoretical limit as conventional IC technology. An E-beam can also be used to directly write patterns onto the flexible masks, making submicron resolution possible.

0-7803-4412-X/98/$10.00 © 1998 IEEE

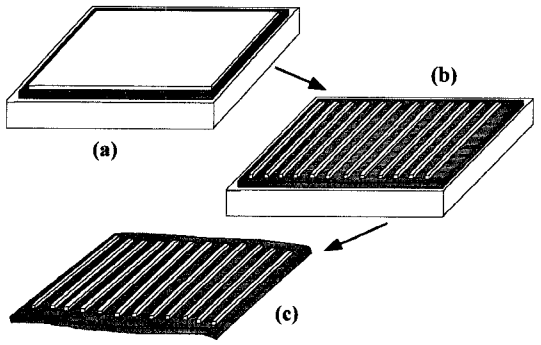

Figure 1. Procedure for making the flexible masks. a) Non-UV-transparent thinfilm can be evaporated onto a flexible material which is then affixed to a rigid substrate before spinning on photoresist. b) Use conventional lithographic techniques to transfer patterns. c) The rigid substrate is removed, leaving a patterned flexible mask.

The major problem encountered during the development of the flexible masks was the cracking in the thinfilm structures on the masks. Mismatch of the expansion coefficients between the thinfilm material and the flexible material was determined to be the primary cause of this problem [11]. This issure was resolved by using an appropriately thick flexible material and minimizing the rigid substrate temperature during thinfilm evaporation.

Photoresist Spraying

Spin coating achieves resist uniformity by balancing two forces: the rotation-induced centrifugal force that drives the flow radially outward, and the resisting viscous force that acts radially inward. Therefore, spin coating will not work for coating cylinders due to the imbalance of centrifugal and viscous forces: the centrifugal force acts in the radial direction while the viscous force acts circumferentially and axially on the cylinder surface. Techniques such as spray-coating, dip-coating, slot-coating, taped-resist, evaporated-resist, and electroplated-resist can be used to coat photoresist onto contoured substrates. We have selected spray-coating to coat the cylinder based on cost and resist thickness considerations. From experiments, the important parameters that govern resist uniformity and thickness are the resist droplet size and the distance of the nozzle from the substrate. The droplet size is controlled by the nitrogen gas pressure, the size of the nozzle outlet, and the viscosity of the photoresist. If these parameters are not optimized, defects in the resist will appear across the substrate. Using AZ5206, resist thickness of 0.6μm with 0.16μm standard deviation can be obtained across the surface of the cylindrical substrates [11]. Using flexible masks, spraying of photoresist, and rotating the substrate during UV exposure, micron-sized structures can be directly patterned onto the surface of a non-planar substrate. Micron-sized structures were successfully patterned onto the surface of a 1.25" diameter, 2" long cylinder as shown in Figure 2.

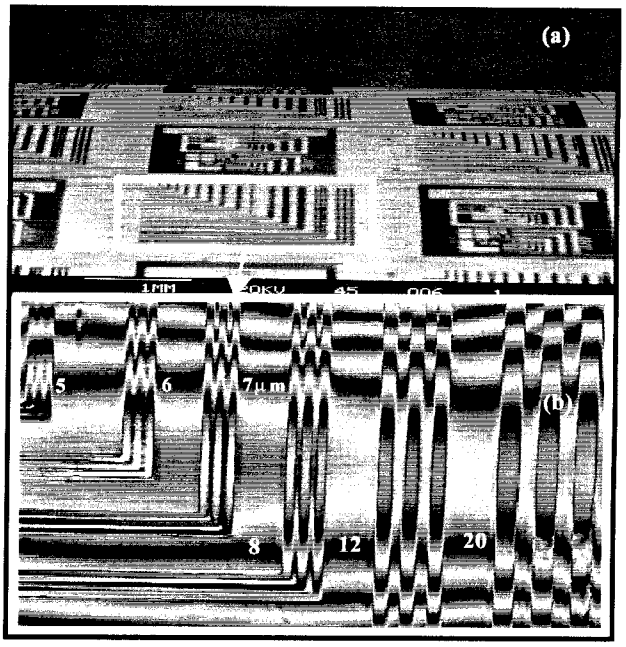

Figure 2. a) SEM picture of Au microstructures on a quartz cylindrical substrate surface. b) Whitelight interferometer image of some width/gap Au structures on the same substrate. The fringes indicate the substrate curvature.

The Customized Alignment System

The three possible alignment errors between patterns on a cylindrical surface and on a flexible mask are shown in Figure 3. In order to correct these errors, two separate alignment systems were built. A yaw-system was used to adjust the relative yaw error. A rotation-translation-system was used to correct the axial and circumferential errors [11].

During the alignment process, the yaw error is first corrected by the yaw-system. Then, the mask is

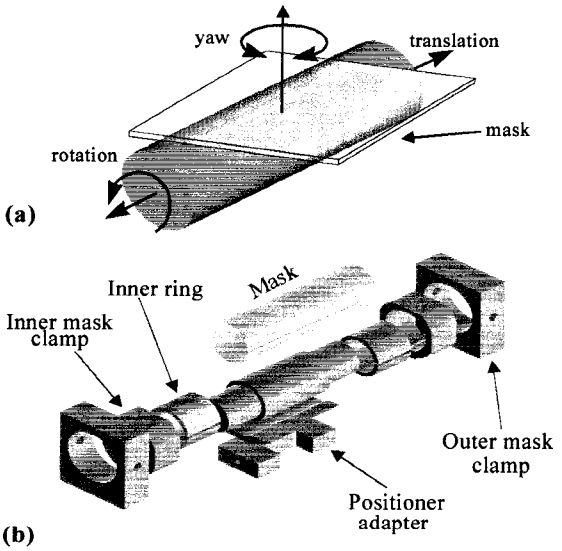

Figure 3. a) The 3 possible misalignment errors. b) Components of the rotation-translation-system.

clamped to the cylinder by a custom-made clamp to fix the yaw position. The mask-cylinder-clamp system is then transferred to the rotation-translation-system for subsequent circumferential and axial error corrections. After the desired alignment is obtained, the mask is made to conformally contact the surface of the cylinder by applying circumferentially distributed radial forces at the ends of the cylinder. An illustration of the rotation-translation system is also shown in Figure 3. The inner mask clamps and rings allow the substrate to translate and rotate relative to the mask. Once the positioning errors are corrected, the outer mask clamps apply uniform radial forces on the mask to conform it to the cylindrical substrate. The current alignment resolution is ~20μm due to excessive stretching of the masks when conformal radial forces are applied.

SACRIFICIALLLY RELEASED STRUCTURES

A fabrication process was developed to create sacrificially release structures that were used as thermal actuators, temperature sensors, and shear stress sensors. This process is briefly described below:

1. Evaporate Cr/Au (300Å/2500Å) onto a quartz cylindrical substrate. The substrate is rotated during evaporation. The quartz cylinder is 2" long and has a 1.25" diameter.
2. Use the FM technique described in the previous section to pattern interconnects and contact pads.
3. Spray AZ5210 photoresist onto the cylindrical substrate. This resist layer is used as the sacrificial material.
4. Evaporate Cr/Au/Ti (300Å/7000Å/1000Å) onto the cylindrical substrate. The structural layers are defined using the FM technique with the customized alignment systems.
5. Sacrificially release the structures by etching the resist layer in a O_2 plasma asher.

Sample structures fabricated successfully using the above process are shown in Figures 4 and 5. The suspended structures shown in Figure 4 were used as temperature and shear stress sensors; the structures shown in Figure 5 were used as thermal actuators. The performance of these sensors and actuators will be presented in the next two sections.

A one-mask process was also developed to sacrificially release Cr/Au structures. The patterned Cr/Au structures can be used to mask the bulk quartz substrate in a 49% HF etch. After sufficient etch time in the HF, over-etch of the bulk quartz material will release the Cr/Au structuresSome samples of bulk-released structures using this wet-release process are shown in Figure 6. These simple structures were also demonstrated as thermal bimorph and lateral actuators.

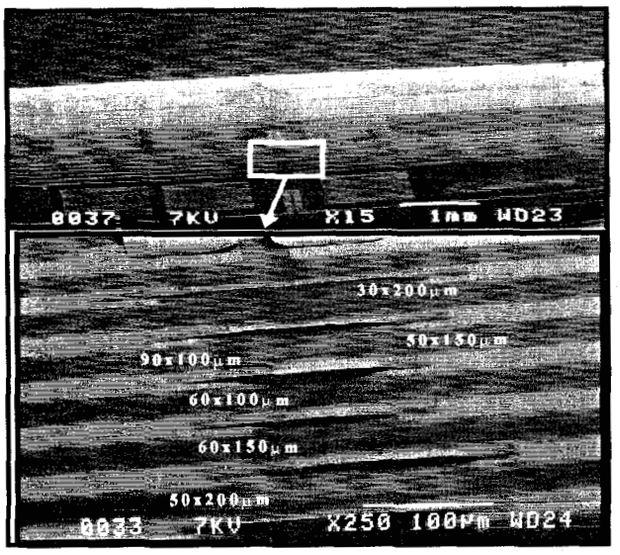

Figure 4. Sacrificially released Cr/Au/Ti structures on the surface of a quartz cylindrical substrate. These structures were used as temperature and shear stress sensors.

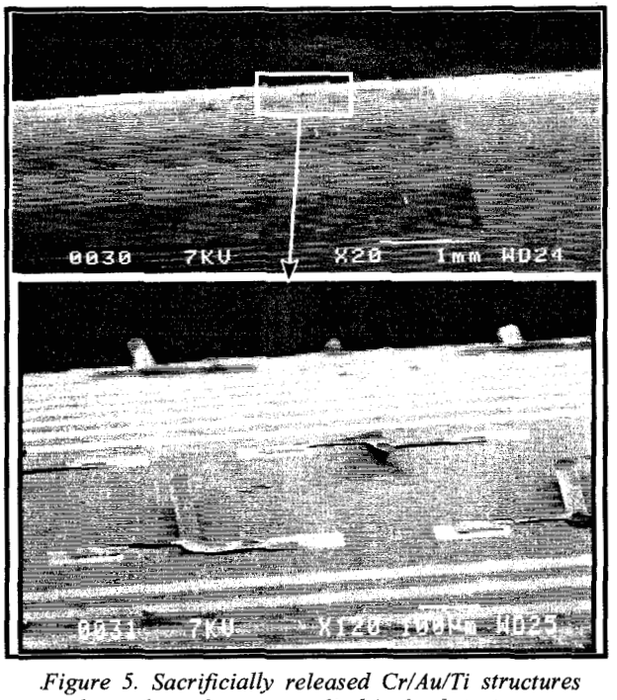

Figure 5. Sacrificially released Cr/Au/Ti structures on the surface of a quartz cylindrical substrate.

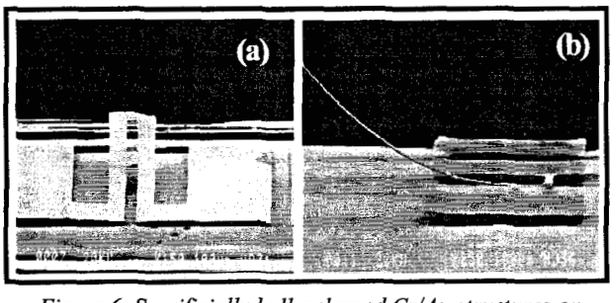

Figure 6. Sacrificially bulk-released Cr/Au structures on the surface of a quartz cylindrical substrate.

THERMAL ACTUATORS ON THE CYLINDRIAL SUBSTRATE

The structures shown in Figures 5 and 6b can be used as lateral thermal actuators. A net lateral motion can be induced at the tip of the long arm by generating thermal strains in the 2 short arms perpendicular to it. As shown in Figure 7, when the arms with lengths L_1 and L_2 are thermally expanded, the long appendage (length L) will deflect to the right. The tip deflection, δ, of the long appendage can be approximated by geometric considerations. If δ is assumed to be small, it can be represented as a function of the thermal strains ε (assume ε_1 and ε_2 are equal):

$$\delta = L\cos\left[\tan^{-1}(d/2\varepsilon)\right] - \varepsilon \qquad \text{Eq. (1)}$$

The thermal strains can be found by multiplying the thermal expansion coefficient, α, with the rise in temperature of the structures, ΔT. The temperature rise in the structures due to resistive heating can be found by invoking the energy conservation law: the rate of energy generated minus the rate of energy leaving a control volume should be equal to the energy stored in the volume. The heat energy generated depends on the current passing through the structures and the electrical resistance of the structures (I^2R); the energy leaving the control volume is due to conduction to the substrate and free convection to the surrounding air. The energy stored depends on the volume, density, and specific heat of the structures. The steady-state solution for the energy balance equation is [12]:

$$\Delta T = I^2R/[hA_1 + KA_2/x] \qquad \text{Eq. (2)}$$

where h and K are the convective and conductive coefficients, respectively; A_1 and A_2 are the corresponding effective areas for conduction and convection, and x is the conduction length. In general, for free convection in air, the conduction term dominates in the above equation if the structural dimensions are in the orders of microns. Then, Eq. (1) can be expressed as:

$$\delta = L\cos\left[\tan^{-1}\left\{d/\left[2\alpha I^2R/(KA_1/x)\right]\right\}\right] - \left[\frac{\alpha I^2R}{KA_1/x}\right] \qquad \text{Eq. (3)}$$

Using the above equation, the theoretical deflections were tabulated and compared to the experimental results as shown in Figure 8. The dimensions of the lateral actuators were L=300μm, L_1=L_2=100μm, d=100μm, and each appendage is 50μm wide. The resistance of these actuators were measured to be ~1Ω, which corresponds to using the averaged resistivity for Au and Ti to calculate the resistance. In the calculation of thermal strain caused by I^2R, the thermal conductivity for quartz (11W/m/°C) was used to determine the conductive heat dissipation. The disagreement between the experimental and theoretical results can be attributed to the crude first-order analysis, i.e., non-temperature dependence of resistivity and small angle approximation of deflections.

THERMAL SENSORS

The suspended bridge structures shown in Figure 4 were

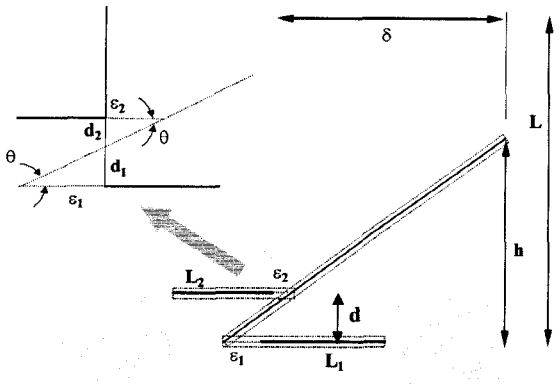

Figure 7. Geometric parameters of the lateral thermal actuators.

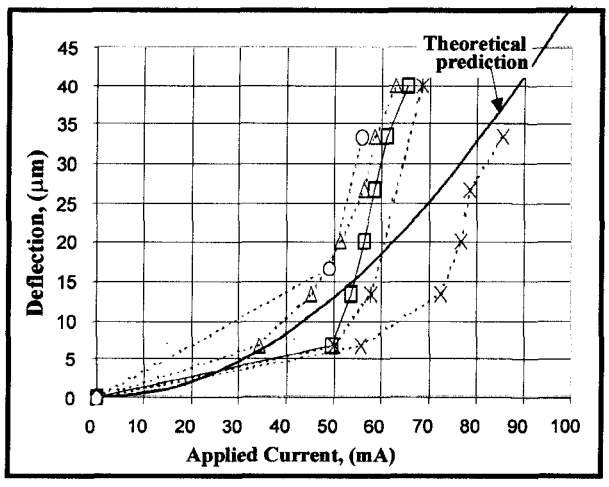

Figure 8. Theoretical calculations are compared with the experimental results for 5 lateral thermal actuators on a quartz cylindrical substrate.

tested as two different types of thermal sensors: temperature and shear stress. The resistance of some resistive materials have a strong dependence on temperature and are, therefore, suitable for use as sensors to detect temperature change. Also, when the temperature of a resistor is elevated by Joule heating, the resistive element can be used as a shear stress sensor. The rate of heat loss from the heated element to the airflow is dependent on the velocity profile inside the boundary layer, and hence, the flow shear stress. The relationship between resistance, temperature, and power input are discussed below.

Temperature Sensors

The resistance, R, of a semiconductor or metal resistive element at a given temperature T is [12]:

$$R(T) = R_o[1 + \alpha(T - T_o)] \qquad \text{Eq. (4)}$$

where R_o is the resistance at room temperature T_o, and β is the temperature coefficient of resistance (TCR). In general, β can also be a function of temperature. Therefore, if T_o, β, and R_o are known, the temperature of the resistor can be determined by measuring the resistance. To determine the TCR of the suspended Cr/Au/Ti elements, the cylinder was packaged as shown in Figure 9. The suspended elements shown in Figure 4 are connected

to 100μm metalization lines that terminate at 2mmX2mm bonding pads. Instead of wirebonding, wire-wrapping wires were initially bonded to the edge of the cylinder by commercial 5min-epoxy. The tips of the wires are then bonded to the boding pads by conductive silver epoxy. The other end of the wires can then be connected to measurement equipment directly.

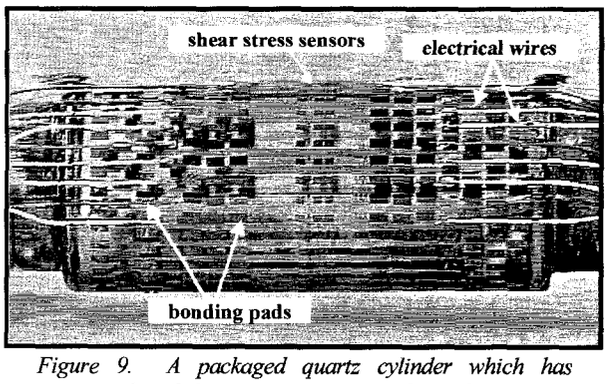

Figure 9. A packaged quartz cylinder which has micromachined shear stress sensors on the surface.

The packaged cylinder was placed in an isothermal oven for TCR measurement. By varying the temperature and measuring the resulting change in sensor resistance, Figure 10 was constructed. The TCR of the bridges were found to ~0.2%/°C as shown in the figure. The averaged known TCR for Cr/Au/Ti is ~0.3%/°C, which is comparable to this measured value.

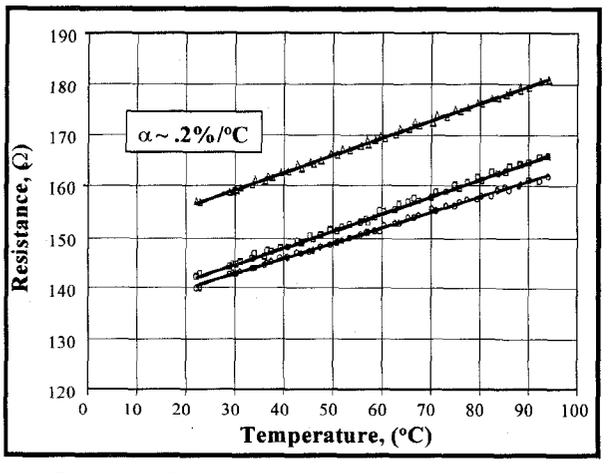

Figure 10. The measured TCR of the Cr/Au/Ti suspended bridges on the surface of a quartz cylindrical substrate.

Shear Stress Sensors

The rate of heat transferred from the resistive element to the flow field depends on the temperature of the resistor and the velocity profile inside the boundary. Therefore, by monitoring the change of the electrical characteristics of the heated resistor, flow shear stress on the surface of a body can be transduced into electrical signal. Using the heat energy balance for a shear stress sensor and Fick's Law of diffusion, the power of a heated resistive sensor can be related to the flow shear stress as [12]:

$$I^2R=\Delta T(A\tau^{1/3}+B) \qquad \text{Eq. (5)}$$

where τ is the shear stress, B is the heat loss due to conduction to the substrate, and A is defined as:

$$A=0.807[CK\rho/L\mu]^{1/3} \qquad \text{Eq. (6)}$$

where C, K, ρ, and μ are the fluid heat capacitance, heat conductance, density, and viscosity, respectively. L is the streamwise length of the heated element. From Equation 5, if a constant current is provided to heat the sensor, the voltage output of the sensor should be proportional to 1/3 power of the flow shear stress. Also from Eq. 5, conduction of heat from the sensor to the substrate must be minimized to maximize the sensitivity of the sensor. Hence, suspending the resistive elements off the substrate is a critical requirement for shear stress measurement.

The cylinder shown in Figure 9 was tested in a windtunnel for shear stress measurement. The cylinder was attached vertically to a rotation platform, as shown in Figure 11, such that sensors can be oriented at different incident angles from the freestream flow. The Pitot was used to calibrate the freestream velocity. Raw output from two different sensors driven with at two different constant currents are shown in Figure 12.

When the 1/3 power of the shear stress (converted from the velocity information) is plotted against the voltage, a linear relation is obtained as shown in Figure 13, which is predicted by Eq. 5.

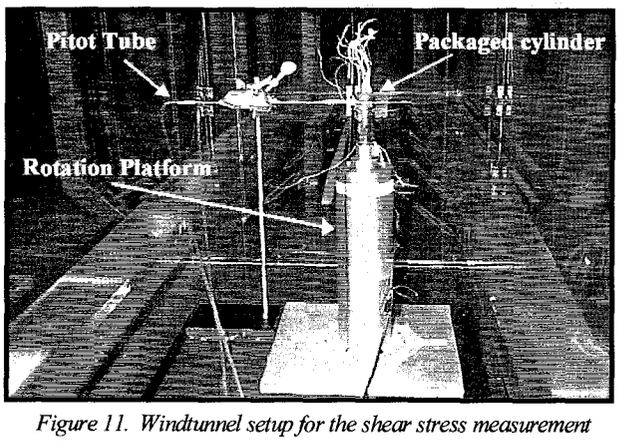

Figure 11. Windtunnel setup for the shear stress measurement using the sensors on the quartz substrate

Flow Separation

The shear stress on the surface of a body depends on the velocity gradient in the boundary layer. The velocity vectors in the boundary layer are initially parallel and uniform in direction at a local point. However, due to kinetic energy loss through friction or the geometry of the body, an adverse pressure gradient is created in the boundary layer. This adverse pressure gradient will cause local flow reversal in the boundary layer. The location in the boundary layer where this flow reversal initially occurs is defined as the separation point. Mathematically, the velocity gradient is zero, and hence, the shear stress is zero at this point. For a cylinder in a laminar freestream flow, separation usually occurs at

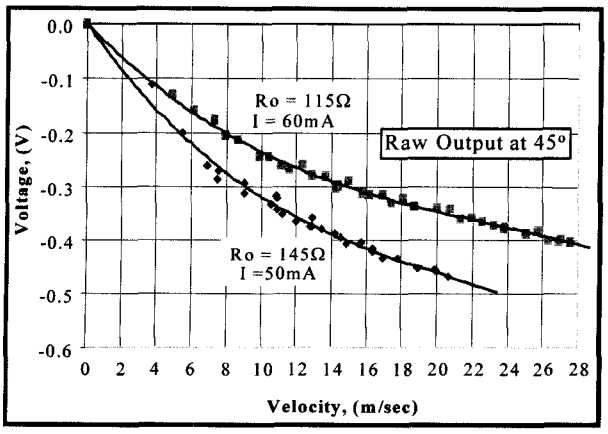

Figure 12. Raw voltage output of the shear stress sensors on a quartz cylindrical substrate.

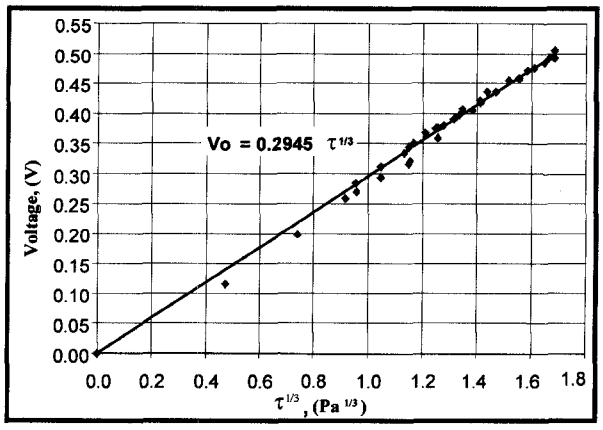

Figure 13. The voltage output the sensors driven with a constant current source is proportional to the 1/3 power of the shear stress.

~80° circumferentially from the flow stagnation point. As shown in Figure 14, the shear stress sensors were used to detect the separation point for different flow Reynolds numbers (velocity dependent). The separation point is indicated by the local minimum voltage output in the figure.

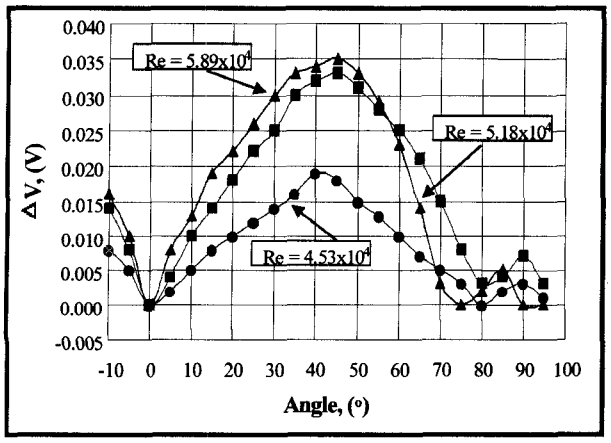

Figure 14. Raw output of shear stress sensors showing a local minimum at θ~80° for various freestream velocities.

CONCLUSION

A novel method was developed to directly fabricate micron-sized structures onto contour surfaces. This method removes the constraint set by the highly developed integrated circuit technology to make micro structures only on planar substrates. Using flexible masks and customized alignment systems, microstructures were built onto 2" long quartz cylindrical substrates that have diameters of 1.25". Presently, 5μm wide structures can be patterned around the surface of quartz cylinders with ~20% yield. The yield increases to ~50% for 10μm structures, ~70% for 20μm structures, and ~90% for structures 30μm and wider.

A dry-release process was developed to sacrificially release metal structures using photoresist as the sacrificial layer. Various microstructures were fabricated on the cylindrical surface and were used as temperature sensors, shear stress sensors, and thermal actuators. The thermal sensors have a TCR of 0.2%/°C. If operated with a constant current source of ~50mA these sensors can be used as shear stress sensors that are able to detect the separation point for flow over a cylinder at Re~$5x10^4$.

We will now proceed to build a system of sensors and actuators to investigate flow control around the cylinder. Suitable thinfilm materials will be used to optimize the performance of these sensors and actuators.

ACKNOWLEDGEMENT

We owe extreme gratitude to Mr. Edward Fortier III for his remarkable technical skills and invaluable suggestions on building and refining the mechanical systems needed for fabrication. Special thanks also to Dr. Tony Tang and Dr. William C. Tang for the usage of the Micro Devices Laboratory equipment at JPL.

REFERENCES

[1] C. M. Ho, et al., *Control of Macro Machine by Micro Actuators*, Bul. of 47th An. Meet. of the Div. of Fluid Dyn. of the APS, Atlanta, Nov. 1994.

[2] B. Gupta et al., *Analog VLSI System for Active Drag Reduction*, IEEE Micro., V. 16, No. 5, pp53-59, 1996.

[3] S. C. Jacobsen and M. Olivier, *Integrated Sensor Network Project, MEMS PI Meet. Rep.* Sarcos Res. Corp., July 1995 – Jan. 1996.

[4] W. F. Dunn, *MEMS-Based Smart Tires, 1st Quart. Tech. Report #GDYR1-15-96S*, The Goodyear Tire & Rubber Comp., Sept. 1995.

[5] Yablonovitch, et al., *Extreme Selectivity in the Lift-off of Epitaxial GaAs Films*, Appl. Phys. Lett., 51(26), 28 Dec. 1987.

[6] G. J. Sullivan, et al., Electron. Lett. 29, p. 1890, 1993.

[7] C. M. Ho, Y. C. Tai, and D. Miu, *Conformable M^3 Microsys. for Aerodyn. Control*, Semi-An. Rep. for ARPA, UCLA/CIT, Jan.-July 1995.

[8] S. C. Jacobsen, et. al., *Fabrication of Micro-Structures Using Non-Planar Lithography*, MEMS91', pp 63-67.

[9] R. J. Jackman et. al., *Fabrication of Submicrometer Features on Curved Substrates by Microcontact Printing*, Science, Vol. 269, 4 Aug., 1995, pp. 665-665.

[10] K. Takahata, et al., *Fine Surface Finishing Method for 3-Dimensional Micro Structures*, MEMS96', pp. 73-78.

[11] W. J. Li and C. M. Ho, *MEMS on Bulk Contour Mechanical Substrates*, Transducers 97', Chicago, June 1997.

[12] W. J. Li, *Ph.D. Dissertation: MEMS on Contoured Substrates*, Nov. 1997, UCLA.